Laser shockwave technique for characterization of nuclear fuel plate interfaces

Perton, M.; Lévesque, D.; Monchalin, J.-P.; Lord, M.; Smith, J. A.; Rabin, B. H.

Publisher's version / Version de l'éditeur:
https://doi.org/10.1063/1.4789068
Review of Progress in Qualitative Nondestructive Evaluation, pp. 345-352, 2012-07-15

LASER SHOCKWAVE TECHNIQUE FOR CHARACTERIZATION OF NUCLEAR FUEL PLATE INTERFACES

M. Perton[1], D. Lévesque[1], J.-P. Monchalin[1], M. Lord[1], J. A. Smith[2], B. H. Rabin[2]

[1]National Research Council Canada, 75 de Mortagne Blvd, Boucherville, Québec, Canada, J4B 6Y4
[2]Idaho National Laboratory, P.O. Box 1625, Idaho Falls, ID 83415-6188 USA

ABSTRACT. The US National Nuclear Security Agency is tasked with minimizing the worldwide use of high-enriched uranium. One aspect of that effort is the conversion of research reactors to monolithic fuel plates of low-enriched uranium. The manufacturing process includes hot isostatic press bonding of an aluminum cladding to the fuel foil. The Laser Shockwave Technique (LST) is here evaluated for characterizing the interface strength of fuel plates using depleted Uranium/Mo foils. LST is a non-contact method that uses lasers for the generation and detection of large amplitude acoustic waves and is therefore well adapted to the quality assurance of this process. Preliminary results show a clear signature of well-bonded and debonded interfaces and the method is able to classify/rank the bond strength of fuel plates prepared under different HIP conditions.

Keywords: Laser Ultrasonics, Shock Waves, Adhesion Testing, Nuclear Fuel Plate
PACS: 62.50.Ef, 68.35.Np, 43.25.Cb, 81.70.Cv, 28.41.Bm

INTRODUCTION

The Global Threat Reduction Initiative (GTRI) of US National Nuclear Security Agency is tasked with minimizing the use of high-enriched uranium (HEU) worldwide. A key component of that effort is the conversion of research reactors from HEU to low-enriched uranium (LEU) fuels. The GTRI Convert Fuel Development program, previously known as the Reduced Enrichment for Research and Test Reactors (RERTR) program, was initiated in 1978 by the Department of Energy (DOE) to develop the nuclear fuels necessary to enable these conversions. The program cooperates with the research reactors' operators to achieve this goal of HEU to LEU conversion without reduction in reactor performance. The GTRI program is currently engaged in the development of a novel nuclear fuel that will enable these conversions. The fuel design is based on a monolithic fuel meat made from a Uranium Molybdenum (U-Mo) alloy foil (typically 0.2 to 0.4 mm) clad in Al-6061, as shown in Fig. 1. This design has shown excellent performance in irradiation testing.

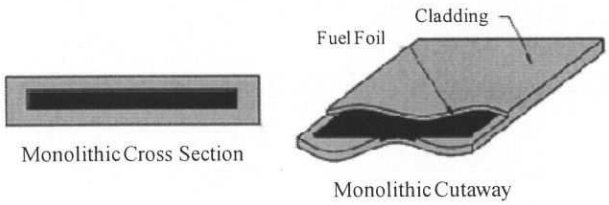

FIGURE 1. Sample geometry.

The development and qualification of monolithic LEU fuel processes are currently being pursued. The initial step in the fabrication process is the development of the LEU-Mo alloy source material that is cast and roll-formed to achieve the required final fuel meat thickness with desired flux profile. Another step includes bonding of the fuel plate aluminum cladding to the foil by hot isostatic pressing (HIP) bonding process. Recent research has been performed to non-destructively characterize bond strength with ultrasonic techniques. In this paper, the Laser Shockwave Technique (LST) is proposed to achieve better performance.

LST has been studied in the past for the measurement of the bond strength of a thin coating on a substrate [1-2]. For these measurements, a high energy pulsed laser is used to generate a high magnitude compression pulse which propagates through the sample. Upon reaching the back free surface, this pulse is reflected as a tensile pulse that can pry off the coating. Recent work addresses the problem of adhesive bonding of thicker structures made of carbon-epoxy composite [3]. In contrast with thin coating, LST does not induce spallation, but only delaminations. One advantage of LST is to provide a local measurement without mechanical contact, which in our case, frees the operator to stay close to the fuel plate for long periods of time. Also there is no crack propagation of the induced debond outside of the test area. The fuel material remains enclosed and the operator is protected against any radioactive hazard that could occur with destructive tests. Another advantage is that the method is not sensitive to specimen geometry and to small surface roughness. However, LST has several distinct characteristics in soliciting the bond quality compared to standard destructive techniques (e.g. the lap shear, double cantilever beam, mixed mode flexure). LST is very high strain rate, and the behavior law is different than under quasi static deformation. The bond strength measured is, in term of critical stress, generally in a ratio of 10 times greater as compared to the static value. Also, the strength measured in LST results from a transient tensile force essentially normal to the interface while standard destructive tests generally imply a large contribution of shear stress.

In this paper, the LST is adapted to the evaluation of bond quality between a depleted uranium (DU) foil and the aluminum cladding by the HIP bonding process. Several conditions of the bonding process are investigated. In the following, the principles of bond strength evaluation are detailed. Results show that the proposed technique is able to differentiate bond quality.

PRINCIPLES AND EXPERIMENTAL APPROACH

A powerful Q-Switched Nd:YAG laser which delivers optical pulses of about 8 ns and a maximum energy of 2 J at 1064 nm wavelength is used to induce shock waves in the DU fuel plates to be tested. The laser beam is focused to a spot diameter of about 3 mm. To avoid surface damage and to increase the efficiency of optical-to-mechanical transduction

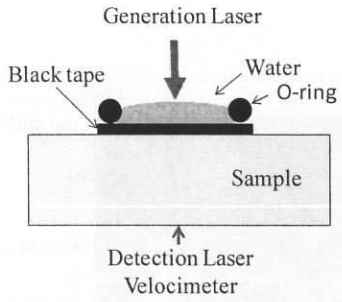

FIGURE 2. Setup for highly efficient shock generation and no damage to the surface: black tape and water.

[2, 3], the surface of the material is first covered with an absorbing tape and then with a constraining medium (such as water), transparent to the laser wavelength, as illustrated in Fig. 2. The waves generated under confinement produce high-amplitude particle displacement compared to ablation of the sample free surface.

The shock wave source size (roughly the laser spot size) is about two times the sample thickness (about 1.5 mm) to be close to a 1D propagation configuration. Consequently, shear stresses are minimized and the generated wave is mostly compressive. This wave is then reflected by the back surface of the plate as a tensile wave. Only the tensile stresses are used to induce a debond at the interface. However, stresses imposed in the material can be the result of several waves, not only the wave reflected from the back surface. To illustrate this point, Fig. 3 shows the time evolution of the stress amplitude in the thickness imposed by an elastic wave pulse generated at the top surface, at time $t = 0$. This result was simulated supposing a 1D propagation model, for thicknesses representative of the fuel plates ($h_1 = 600$ µm, $h_2 = 280$ µm, $h_3 = 510$ µm) and with typical velocity values of the longitudinal mode (aluminum: $c_{Al} = 6400$ m/s and DU: $c_{DU} = 2400$ m/s). The top surface is defined here as the surface where the shock is produced. The interface between the top (resp. the bottom) aluminum layer and the DU foil is denoted I_1 (resp. I_2). The temporal profile of the pulse, represented by the offset triangle in Fig. 3, is assumed triangular and of duration T, with a sharp compression front and a slow release (rarefaction), in close agreement with previously measured loading [3]. Due to the reflections at the interfaces or surfaces, other tensile waves arise and cumulative effects imply large tensile stress concentration at the interfaces. The cumulative effects are important in this case due to the fact that the propagation times in any of the three layers are almost equal.

The bond strength is determined by increasing the laser pulse energy step by step and corresponds to the ultimate stress value imposed at the interface, i.e. the stress at which debond occurs. To limit cumulative effects of plastic deformation in the materials, a single shock is applied at each location. In fact, since the waves are reflected on each surface or interface, they propagate in a medium that is already subject to plastic deformation and therefore cumulative effects occur during a single shock. That is why even if the joint remains closed after a single shock, the joint could have been weakened. To correctly evaluate the bond strength, cumulative effects should be minimized and only debonds occurring from the first arrival of a tensile wave at an interface (t_{r1}, or t_{r2} in Fig. 3) are considered. This requires that the effects of transient stresses are evaluated in real time during the shock propagation. This is achieved indirectly by monitoring the back-wall surface velocity u by a second laser and an optical velocimeter based on a solid Fabry-Perot etalon (see Fig. 2). The second laser is a long pulse (>120 µs) Nd:YAG, operated at 1064 nm wavelength. A detailed description of the etalon interferometer can be found in reference [4].

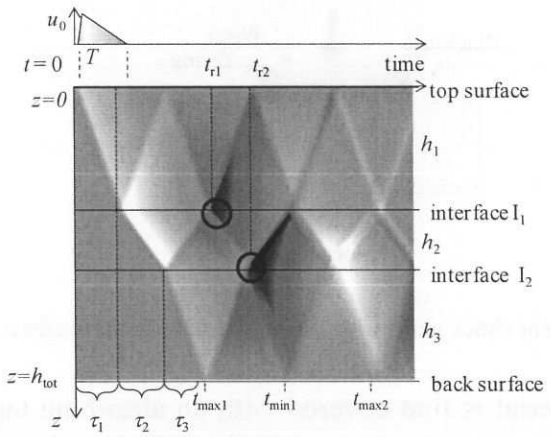

FIGURE 3. Time-space diagram of the propagation of a shock wave pulse with duration T. White and black areas represent respectively the compression wave (pressure above the average pressure) and the tensile wave (pressure below the average pressure).

The relation between the back-wall surface velocity and the in-depth stress is calculated from the propagation and back-propagation of the waves that reached the back surface up to the desired depth. For that purpose, one has the simple relation between the particle velocity at a depth z and time t, and the back surface velocity imposed by a wave assuming 1D elastic propagation in a homogeneous material without attenuation:

$$u(z,t)=1/2\left(u(h_{tot},t-z'/c)+u(h_{tot},t+z'/c)\right), \qquad (1)$$

with $h_{tot}=h_1+h_2+h_3$, c the wave propagation velocity and $z'=h_{tot}-z$. The term $u(h_{tot},t-z'/c)$ corresponds to the contribution that will arrive at time t at depth z' from the back surface, and the term $u(h_{tot},t+z'/c)$ is the contribution present at time t and at depth z' that is propagating toward the back surface. The factor $1/2$ comes from the total reflection at the free surface. Then, the relation between the particle velocity and the stress σ inside the plate is given by:

$$\sigma(z,t)=\rho c u(z,t) \qquad (2)$$

where ρ is the material density.

The relations for a multilayer are a bit more complicated, and clearly worse when plastic deformation and plastic hardening occur [5]. Here, stresses at the interfaces are evaluated under the elastic propagation assumption. Nevertheless, part of the plastic effect is taken into account by using the signal recorded at the back surface. Also, since the geometry and material are identical for all fuel plates, the plastic effect should not change the ranking of bond strengths between tested samples. Also, one should note that a simple classification as function of the laser power cannot be used with the current setup. In practice, about 20% variation of the laser power is observed between consecutive shots. Also, since the water confinement thickness is not precisely controlled, optical absorption of the incident light may vary. Finally, the transmission of the wave through the interface between the tape and the sample depends on the adhesive bond quality, and some variability is thus expected.

The stress evaluation based on the back surface velocity is then the most appropriate. The stress at the first interface at time t_{r1} is calculated from the particle velocities of the three waves present at that time and that position (see Fig. 3):

$$\sigma(h_1,t_{r1})=\rho_2 c_2 u_{01}(t_{r1},h_1)+\rho_1 c_1 u_{0121}(t_{r1},h_1)+\rho_2 c_2 u_{0101}(t_{r1},h_1) \qquad (3)$$

where u_{01}, u_{0121} and u_{0101} refer to the waves that propagated from the top surface to the interface I_1, after a path with reflection or transmission at the interfaces or surfaces indicated by the indices 0, 1, 2, 3, respectively the top surface, the interfaces I_1, I_2 and the back surface. One should first deduce the particle velocity of the wave generated at the top surface (u_0) from the back-propagation (division by reflection or transmission coefficient and negative time shift) of the amplitude, u, observed at the back surface. Then, the particle velocities u_{01}, u_{0121} and u_{0101} are calculated from the propagation (multiplication by reflection or transmission coefficient and positive time shift). With the travel times (τ_1, τ_2, τ_3) in the different plates defined in Fig. 3, the stress at the first interface becomes:

$$\sigma(h_1,t_{r1})=\frac{1}{2T_{23}^P}\rho_3 c_3\begin{pmatrix}u(t_{r1}+\tau_2+\tau_3)+R_{23}^P T_{21}^P u(t_{r1}-\tau_2+\tau_3)\\-R_{12}^P u(t_{r1}-2\tau_1+\tau_2+\tau_3)\end{pmatrix} \quad (4)$$

The amplitude of the generated wave can only be deduced easily at time before t_{min1} in Fig. 3. This time corresponds to the minimum in the back surface velocity signal, which is due to the first arrival of the several tensile waves. The presence on the back surface of other wave arrivals after this moment does not allow identifying its amplitude from the total surface velocity. That is why the contribution of $u(t_{r1}+\tau_2+\tau_3)$, where $t_{r1}+\tau_2+\tau_3>t_{min1}$, is not taken into account. However this simplification is acceptable since the amplitude of the generated wave at time $t_{r1}-\tau_1>T$ can be considered negligible. The pressure at the second interface and at time t_{r2} is calculated in the same way:

$$\begin{aligned}\sigma(h_1+h_2,t_{r2})&=\frac{1}{2}(\rho_3 c_3 u_{012}+\rho_2 c_2 u_{01232}+\rho_3 c_3 u_{01012}+\rho_3 c_3 u_{01212})(t_{r2},h_1+h_2)\\&=\frac{1}{2}\rho_3 c_3\begin{pmatrix}u(t_{r2}+\tau_3)-T_{32}^P u(t_{r2}-\tau_3)+\\-R_{12}^P u(t_{r2}-2\tau_2+\tau_3)+R_{23}^P R_{21}^P u(t_{r2}-2\tau_1+\tau_3)\end{pmatrix}\end{aligned} \quad (5)$$

Note that one considers here a perfect transmission through I_1, assuming no debond at the first interface.

In addition, laser-ultrasonic measurements made prior and after laser shocks are used to confirm the presence, to determine size and to locate depth of debonds. These measurements consist in a scan obtained from another experimental setup, where generation and detection spots are on the same surface, superimposed, with diameter sizes of about 1 mm and 0.5 mm, respectively. The step size of the scan is 0.5 mm in both directions on the sample surface. The generation laser was a Nd:YAG, operated at 355 nm wavelength with a FWHM of 35 ps. The energy was about 6 mJ, just above the ablation threshold. The detection uses a long pulse (>120 µs) Nd:YAG laser, operated at 1064 nm wavelength and a photorefractive interferometer. Also note that the laser-ultrasonic inspection is performed without the tape or water confinement.

RESULTS

Velocity signal description

The Fig. 4a shows the typical back surface velocity signal for three laser energies, starting from a value well below any damage, to values right above the debond threshold of interfaces I_1 and I_2. As already mentioned, the laser energy should only be considered as an indication and only one shock was applied at each location.

The first acoustic pulse, between 300 µs and 450 µs corresponds to the generated wave that crosses the entire sample and arrived at time t_{max1} in Fig. 3. A small step at about 10 m/s, denoted HEL_1, corresponds to the aluminum Hugoniot Elastic Limit, i.e. the threshold between elastic and plastic behavior in aluminum at high strain rate. Another step at about 25 m/s, denoted HEL_2, is expected to correspond to the DU HEL. The front waves below HEL_1 are similar for all laser energies and correspond to the so-called precursor which propagates with the elastic velocity. Behind these front waves follow a larger amplitude signal that evolves considerably with the laser energy. This corresponds to the so-called "plastic wave" which is associated to the plastic deformation. The wave propagation is therefore in the "elastic-plastic regime" [5, 6, 7]. These experiments are thus well suited to characterize at high strain rate, from the deformed temporal shape of the pulse, elastic and non-elastic material properties such as yielding, strain hardening, viscoplastic flow [5]. Also, one should note that other smaller non-linear effects come from the generation mechanism itself, i.e. the ablation in a constrained medium, or from the shock propagation where the wave propagation velocity is dependent of the local pressure. The particle velocity signals were all recorded for the same plate thickness, so that the non-linearity effects on the pulse shape are easy to visualize as a function of the laser energy in Fig. 4a. Nevertheless, one should note that the non-linearities occur during propagation, so that the shape of a pulse observed at the back surface can be different from the shape at a different depth. These effects are not considered in the present stress evaluation.

For the signal obtained under 400 mJ laser energy, the compression pulse (positive velocity signal) is then followed by a tensile pulse (negative velocity signal between 450 µs and 650 µs) which corresponds to the sum of three waves, each undergoing two reflections inside any one of the three plates (arrivals around t_{min1} in Fig. 3). When the signals are normalized, Fig. 4b, distinct signatures (indicated by arrows in Fig. 4b) are observed for the two signals at larger laser energies, attributed to interface debond that changes the reflection conditions.

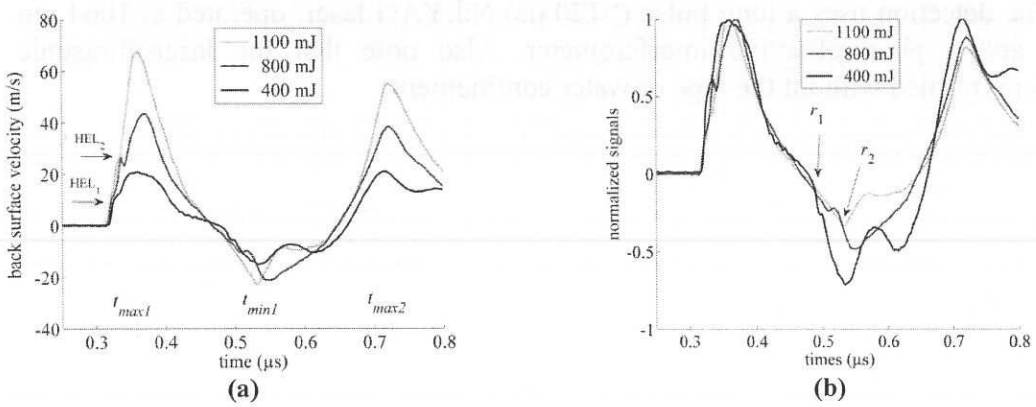

FIGURE 4. **(a)** Back surface velocity signals measured for laser shock pulse energies below any interface debond (400 mJ), at interface I_1 (800 mJ) and I_2 (1100 mJ) rupture thresholds. (b) Same signals normalized.

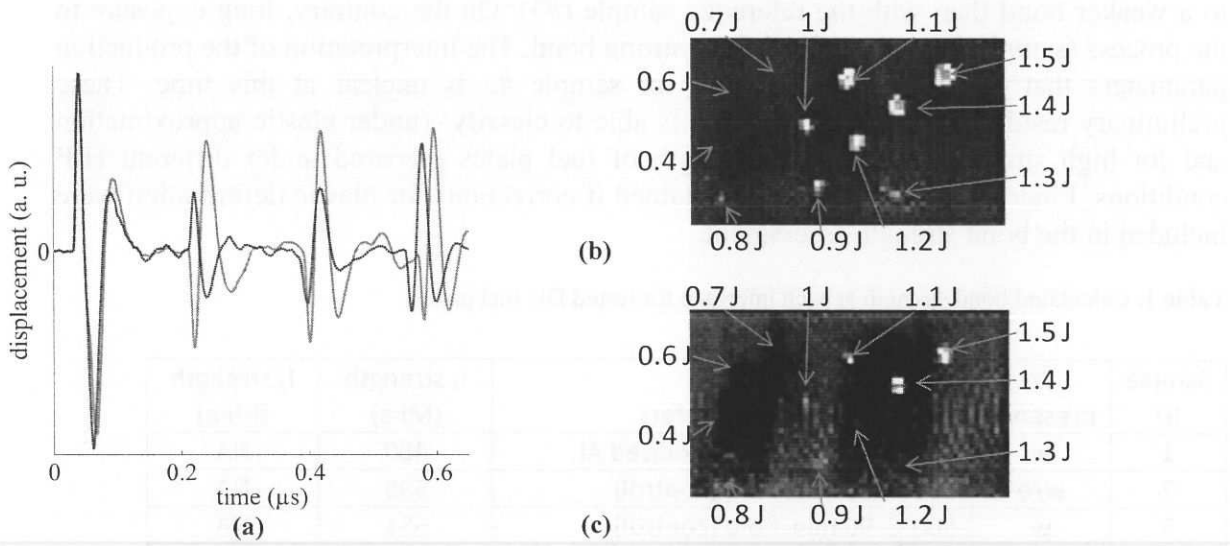

FIGURE 5. (a) Typical signals in a sound area (black) and in a debonded area (gray). C-scans from (b) top surface and (c) back surface on sample #3.

Bond strength results

Four laser-ultrasonic scans were realized for each DU fuel plate, before and after shocks and from both sides (top and bottom surfaces). A typical signal obtained during the scan before shock (black signal), filtered between 10 and 80 MHz, is presented in Fig. 5a. It is taken from the sound area as a reference. Another signal (gray signal) typical from a debonded area is also presented. The second echo, between 0.15 and 0.30 μs in the signals, corresponds to the surface displacement imposed by the wave reflected on the first interface, I_1 or I_2 depending on which side the scan is realized. Travel times τ_1, τ_2, τ_3 are also deduced from these signals.

The C-scans presented in Fig. 5b and 5c were obtained by making the cross-correlation of the second echo obtained from the post-shock laser-ultrasonic scans, with the second echo of the reference signal shown in Fig. 5a. The black color corresponds to a correlation coefficient above 0.9 while the white color denotes a correlation coefficient below -0.9. The white spots then represent the areas where the echoes are inverted, corresponding to a reflection on a debonded free surface. The results in Fig. 5b and 5c demonstrate that both interfaces can be debonded during a single shock. Also, a lower laser energy is needed for the debond of interface I_1 compared to interface I_2. But, since the laser energy is not a good indication of the in-depth stress, one should refer to the stress calculated from eqs (4) and (5). Also, it is reminded that since the rupture at I_2 occurs after the one at I_1, the stress at I_2 is much lower than shown in Fig. 3.

As summarized in table 1, several conditions of the HIP bonding process have been tested, such as the influence of the temperature, the duration of the process, the presence or absence of a zirconium film around the DU foil or of oxidized aluminum plates. In contrast to other samples tested, eq. 5 was used for sample 5, where one debond at interface I_2 had been observed from the back surface without being observed from top surface. The reason for this different behaviour is due to a smaller thickness of h_3. At higher laser energy, both interfaces were debonded, allowing determining the bond strength also for interface I_1. As expected, the two interfaces for this sample exhibit almost same bond strength. Also, the presence of oxidized aluminum (sample #1) or the absence of zirconium (sample #2) leads

to a weaker bond than with the reference sample (#3). On the contrary, long exposure to the process (sample #4) is beneficial for a strong bond. The interpretation of the production parameters that lead to higher strength for sample #5 is unclear at this time. These preliminary results show that the method is able to classify -(under elastic approximation and for high strain rate) the bond strength of fuel plates prepared under different HIP conditions. Finer results could also be obtained if corrections for plastic deformation were included in the bond strength assessment.

Table 1. Calculated bond strength at each interface for tested DU fuel plates.

Sample ID	Zr presence	HIP parameters	I_1 strength (MPa)	I_2 strength (MPa)
1	w	560°C, 60 min. hold, oxidized Al	480	NA
2	w/o	560°C, 90 min. hold (control)	595	NA
3	w	560°C, 90 min. hold (control)	651	NA
4	w	560°C, 345 min. hold	765	NA
5	w	520°C, 90 min. hold	1045	1000

CONCLUSIONS

A LST method based on high-intensity laser shock waves combined with laser-ultrasonic inspection has been used to test the bond strength between DU foil and aluminum cladding in fuel plates. Several conditions of the HIP bonding process have been tested, such as the influence of the temperature, the duration of the process, the presence or absence of a zirconium film around the DU foil or of oxidized aluminum plates. These preliminary results show that the velocimeter signal gives signatures of well-bonded and debonded interfaces and that the method is able to classify the bond strength of fuel plates prepared under different HIP conditions. Finer quantitative results, under high strain rate, could also be obtained if corrections or calibration for plastic deformation were included in the bond strength assessment. The method can be thus made quantitative and in-situ for fabrication of monolithic LEU fuel.

REFERENCES

1. J. L. Vossen, ASTMM Spec. Tech. Publ., **640**, pp. 122-131 (1978).
2. J. Yuan, V. Gupta, A. Pronin, *J. Appl. Phys.* **74,** pp. 2405-2410 (1993).
3. M. Perton, A. Blouin and J.-P. Monchalin, *J. Phys. D: Appl. Phys.* 44 (2011)
4. M. Arrigoni, J.-P. Monchalin, A. Blouin, S. E. Kruger and M. Lord, *Meas. Sci. Technol.* **20**, 015302 (7pp) (2009).
5. L. Davison, D. E. Grady, M. Shahinpoor, *High-Pressure Shock Compression of Solids II*, Springer-Verlag, New York (1996).
6. J. R. Asay, M. Shahinpoor, *High-Pressure Shock Compression of Solids*, Springer-Verlag, New York 1993.
7. R. A. Graham, Solids Under High-Pressure Shock Compression, Springer-Verlag, New York (1993).